ELSEVIER

Earth and Planetary Science Letters 178 (2000) 39–46

EPSL

www.elsevier.com/locate/epsl

Profiles of the Bullen parameter from mantle convection modelling

Ctirad Matyska [a,*], David A. Yuen [b]

[a] Department of Geophysics, Faculty of Mathematics and Physics, Charles University, V Holešovičkách 2, 180 00 Prague 8, Czech Republic

[b] Department of Geology and Geophysics and Minnesota Supercomputer Institute, University of Minnesota, Minneapolis, MN 55415-1227, USA

Received 15 November 1999; received in revised form 22 February 2000; accepted 22 February 2000

Abstract

The state of adiabaticity in the mantle can be assessed by using the Bullen parameter profile derived from seismology. We have employed the extended-Boussinesq convection models in a cartesian 2-D domain to extract the Bullen parameter as a function of depth in both base heated and internally heated configurations and for both constant and variable thermal conductivity. We also studied models with depth-dependent thermal expansivity. Our results show that the values of the Bullen parameter for a Rayleigh number of 10^6 lie close to one, with sometimes excursions out to 0.9 and 1.1. They are sensitive to the mode of heating and the depth dependences of the thermal expansivity and changes of thermal conductivity. We obtained a subadiabatic geotherm above the lower boundary layer in all the models with constant thermal expansivity but a decrease of thermal expansivity with depth can result in a subadiabatic geotherm below the upper boundary layer. Thus the profiles of the Bullen parameter have a definite potential of being useful in constraining the physical parameters and flow structures associated with mantle convection.

Keywords: thermodynamic properties; numerical models; geothermal gradient; mantle; convection

1. Introduction

The adiabatic state in the mantle is a general assumption commonly made in geophysics, because of the seemingly high vigor of mantle convection, which has been accorded the status of being in a highly supercritical state. Whether or not the mantle is adiabatic is important for several reasons: (i) for the mode of heat transport and consequences on thermal history, (ii) geochemistry and chemical stratification in the mantle, and (iii) mineral physical state, elastic constants and issues of metastability in phase transitions. The observations of the periods of free oscillation can provide direct constraints on the size of departures from a state of chemical homogeneity and adiabaticity [1]. The adiabatic state is commonly assumed in thermodynamic cal-

* Corresponding author. Tel.: +420-2-21912538; Fax: +420-2-21912555; E-mail: ctirad.matyska@mff.cuni.cz

0012-821X/00/$ – see front matter
PII: S0012-821X(00)00060-1

culations for the equation of state parameters [2], such as the derivatives of the elastic parameters [3]. Many mineral physicists have favored the idea of an adiabatic lower mantle [2,4] and used this concept in determining equation of state parameters.

It is well known from basic seismology (e.g. [5]) that the Bullen parameter, η, yields important information concerning the condition of adiabaticity in a dynamic mantle and regions in the Earth where there may be significant deviations from the adiabatic state, as in the D″ layer above the core–mantle boundary (CMB) [6] and the lithospheric boundary layer. Steinbach and Yuen [7] have found by using passive tracers that inside plumes and downwellings there are regions with both subadiabatic and superadiabatic tendencies, because of the nature of time-dependent convection. Yet there has been no work up to now on extracting the profiles of the Bullen parameter from the output of mantle convection models. The reason for this is probably the prevalent usage of the Boussinesq models in convection, where the local adiabat is not explicitly included in the temperature equation. Therefore, in order to obtain η under more realistic circumstances, one must use either the extended-Boussinesq (e.g. [8]) or the anelastic fluid model (e.g. [9]) for portraying mantle convection. However, there is no substantial difference between the two approximations [10]. Although these extra-Boussinesq models have been around for more than a quarter of a century [11], they have not been employed a great deal with few exceptions, because of the influences of laboratory models of mantle convection [12], which are inherently Boussinesq in nature because of the extremely thin layer of the working fluid in the laboratory apparatus.

In this paper we will employ the extended-Boussinesq convection model to calculate the Bullen parameter for different earth models. In particular, we will draw attention to the effects arising from the decrease of thermal expansivity with depth [13], the new variable thermal conductivity model [14], and internal heating, since the amount of internal heating in the lower mantle has also been raised recently by a new chemically stratified model [15].

2. Model description

For the purpose of illustrating the basic physics of convection with variable thermal conductivity, depth-dependent thermal expansivity, and internal heating, a model consisting of a 2-D rectangular box with an aspect ratio of four has been adopted. The momentum and thermal equations for extended-Boussinesq fluid with neglected inertial forces (e.g. [8]) and for impermeable and free-slip boundary conditions were solved, i.e. we are dealing with the system:

$$\nabla \cdot \mathbf{v} = 0 \tag{1}$$

$$\nabla^2 \mathbf{v} - Ra\ \alpha T \mathbf{e}_z - \nabla p = 0 \tag{2}$$

$$\frac{\partial T}{\partial t} = \nabla \cdot (k \nabla T) - \mathbf{v} \cdot \nabla T + R - D\alpha \left(T + \frac{T_0}{\Delta T} \right) v_z + \frac{D}{Ra} \left(\nabla \mathbf{v} + (\nabla \mathbf{v})^T \right) : \nabla \mathbf{v} \tag{3}$$

where $\mathbf{v} = (v_x, v_z)$, T and T_0 are, respectively, dimensionless velocity, temperature and surface temperature, p is the dimensionless dynamical pressure, $\mathbf{e}_z$ is the unit vector pointing downward, t is the dimensionless time, k is the dimensionless thermal conductivity normalized by k_s and α is the dimensionless thermal expansivity normalized by α_s. The symbol ':' represents the total scalar product of two tensors and the superscript 'T' denotes the transposition.

This dimensionless non-linear evolutionary system of equations is controlled by the Rayleigh number $Ra = \rho^2{}_s c_p \alpha_s \Delta T g d^3 / \zeta_s k_s$ (ρ_s is a reference density, c_p is the specific heat under a constant pressure, ΔT is the temperature drop over the mantle, g is the gravity acceleration, d is the mantle thickness and ζ_s represents a reference dynamic viscosity) and by the internal heating number $R = Qd^2 / k_s \Delta T$ (Q denotes volumetric heat sources). A value of $R = 12$–15 corresponds to the magnitude of chondritic heating. The last controlling parameters are the dissipation number $D = \alpha_s g d / c_p$ and the forms of k and α. The Rayleigh number $Ra = 10^6$ and the dissipation number

$D = 0.5$ [13] were chosen as fixed parameters in this study.

The stream function formulation $v_x = \partial\psi/\partial z$, $v_z = -\partial\psi/\partial x$ was employed to satisfy automatically the condition in Eq. 1. The spatial derivatives in Eqs. 2 and 3 were performed by an eighth-order difference scheme [16] employing 512×128 grid points for the heat equation (Eq. 3) and a coarser grid (by a factor of four along each direction) to discretize the momentum (Eq. 2). Time-stepping was carried out with a second-order explicit Runge–Kutta scheme.

To test the influence of variable thermal conductivity on the mantle geotherm, we have performed numerical experiments with constant thermal conductivity ($k = 1$) as well as thermal expansivity ($\alpha = 1$) and, following Hofmeister [14], we compared them with those for:

$$k(z,T) = [1.0 + 2.5z]\left(\frac{T_0}{T_0 + T}\right)^{0.3} \exp(-0.447T) + 1.03(T_0 + T)^3 \quad (4)$$

where $z \in \langle 0, 1\rangle$ is the dimensionless depth. The first term yields the estimate of pressure and temperature dependence of the lattice thermal conductivity, whereas the second term corresponds to radiative transfer of heat. As $T = 0$ at the surface $z = 0$, Eq. 4 means that the reference thermal conductivity k_s coincides with the surface lattice contribution. This dimensionless formula was derived from that by Hofmeister [14] by assuming the values $\alpha_s = 3\times10^{-5}$ K^{-1}, $\Delta T = 3725$ K, the Grüneisen parameter of 1 and the bulk modulus and its pressure derivative, which are characteristic for perovskite [14]. We used the expression for radiative thermal conductivity, where it is dependent on the cube of temperature. The consequence is that only for temperatures close to the CMB temperature, radiative transfer of heat can play an important role. We are aware of the fact, pointed out by Hofmeister [14], that for low temperatures, lower than 2500 K, the dependence of radiative conductivity on temperature may be more complex, due to the presence of iron in the mantle mineral assemblages.

Finally, we also tested the influence of variable thermal expansivity $\alpha(z)$. Following Chopelas and Boehler [17] and Hansen et al. [13] we have performed the simulations with $k = 1$ and:

$$\alpha(z) = \frac{8}{(2 + z)^3} \quad (5)$$

which yields a decrease of α across the layer to 30% of its surface value.

To evaluate the Bullen parameter η, we follow Poirier ([18], pp. 197–199). We start off with the extended Adams–Williamson equation:

$$\frac{d\rho}{dz'} = \frac{\rho g}{\Phi} - \alpha'(z)\rho\left(\frac{dT'}{dz'} - \frac{\alpha'(z)gT'}{c_p}\right) \quad (6)$$

where the prime is used to distinguish dimensional quantities and $\Phi = v_P^2 - \frac{4}{3}v_S^2$ is the seismic parameter (v_P and v_S are the P and S wave velocities). We recall that $\alpha'(z)gT'/c_p$ is the adiabatic gradient and thus the extended Adams–Williamson equation takes into account density variations due to thermal expansion. The Bullen parameter represents the ratio between $d\rho/dz'$ and the adiabatic density gradient $\rho g/\Phi$, i.e.:

$$\eta = 1 - \frac{\alpha'(z)\Phi}{g}\left(\frac{dT'}{dz'} - \frac{\alpha'(z)gT'}{c_p}\right) \quad (7)$$

Returning to dimensionless quantities, we can rewrite this expression as:

$$\eta = 1 - \frac{\alpha_s\alpha(z)\Phi\Delta T}{gd}\left(\frac{dT}{dz} - D\alpha(z)(T_0 + T)\right) \quad (8)$$

We have used the constant values, surface value of thermal expansivity $\alpha_s = 3\times10^{-5}$ K^{-1}, $\Delta T =$ 3725 K, $g = 10$ m s^{-2}, $d = 2890$ km and $\Phi = 90$ km^2/s^2, which corresponds to the PREM value in the midmantle at a depth of around 1500 km [19]. For estimating dT/dz and T, we have first averaged over the horizontal coordinate the 2-D temperature fields obtained from the numerical modelling. The geotherm provided by this averaging is denoted by $\langle T\rangle(z)$. Since seismic models have finite resolution in the lower mantle of the order of several hundred kilometers in depth [20–22], we then averaged $d\langle T\rangle/dz$ and $\langle T\rangle$ over a depth interval $\langle z-0.05, z+0.05\rangle$ (this corresponds to a layer of thickness about 300 km) to evaluate η in depth z. The effect of the spatial averaging is to reduce the fluctuations of η. This approach to evaluating $\eta(z)$ makes it possible, in principle, to compare convection models with seismic models without requirement of a high resolution. A subadiabatic state is denoted by $\eta > 1$ and a superadiabatic state by $\eta < 1$. Boundary layers are characterized by values of η substantially smaller than 0.9, i.e. very superadiabatic.

3. Results

In Fig. 1 we show the profiles for the horizontally averaged temperature $\langle T\rangle(z)$ and for the Bullen parameter $\eta(z)$ for constant conductivity and purely basal heating mode. The profiles are displayed at three time instants with sufficiently long intervals of time difference Δt around 0.01, i.e. of the order of 10^9 years. We can thus get a good estimate of possible fluctuations of considered quantities due to the non-stationarity of the non-linear convective system being studied. We note that η is more sensitive to the time dependence of mantle convection than $\langle T\rangle$ because of the composite nature of Eq. 8, which represents a local balance between two dynamically varying quantities $\langle T\rangle$ and $d\langle T\rangle/dz$.

Near the surface and the CMB, η, being less than 1, displays a strongly superadiabatic character, as expected because of the presence of the boundary layers at these two depths. In the upper part of the layer η hovers around the adiabatic value, i.e. $\eta \doteq 1$. The fluctuations are smaller in the upper part than in the deep mantle, where values of η higher than 1.15–1.2 can be attained. Such high values may be detectable with current high-resolution tomographic models [22]. The physical reason why there is a remarkable difference between upper and lower parts of the model is the presence of viscous dissipation and adiabatic heating/cooling, which acts differently in cold downwellings and hot upwellings. The classical Boussinesq approximation ($D = 0$) cannot yield such a systematic asymmetry in the vertical boundary layers because of the full symmetry between hot and cold vertical flows.

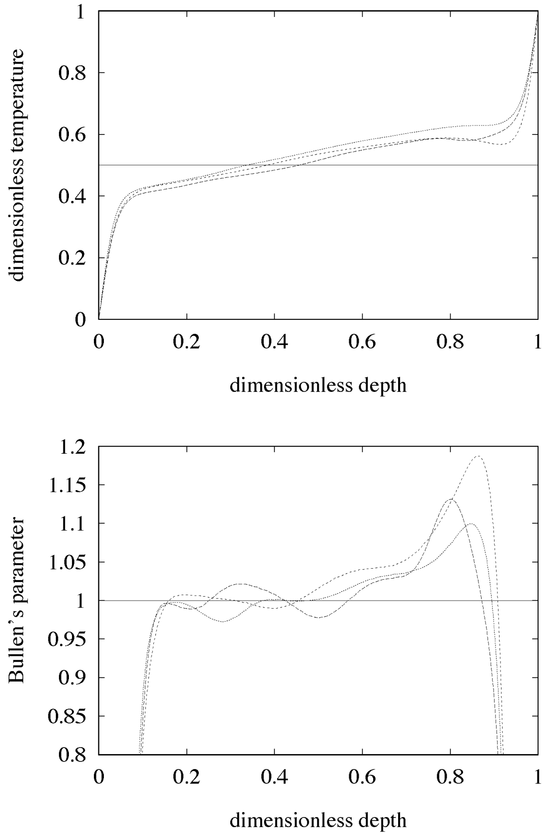

Fig. 1. Three snapshots of dimensionless horizontally averaged temperature $\langle T\rangle$ and the Bullen parameter η as a function of dimensionless depth z for the constant thermal conductivity $k = 1$, constant thermal expansivity $\alpha = 1$ and purely basal heating $R = 0$. To obtain $\eta(z)$ we averaged dT/dz and T over the interval $\langle z-0.05, z+0.05\rangle$, which corresponds to 300 km in the Earth's mantle.

Fig. 2 shows $\langle T\rangle$ and η for bimodal heating with an internal heating rate of $R = 8$. One can clearly recognize that smaller excursions into subadiabaticity in the deep mantle are found for this bimodal heating model. On the other hand, a slightly subadiabatic profile is also typical for depths below the upper boundary layer.

Three-dimensional convection calculations [23] have found that the interior of the mantle is hotter with variable thermal conductivity for both Boussinesq and the extended-Boussinesq approximations. This increase in temperature in turn would boost the adiabatic temperature gradient. Fig. 3 displays the corresponding profiles of $\langle T \rangle$ and η for variable thermal conductivity and $R=0$, whereas Fig. 4 corresponds to the case with $R=8$. Temperatures are greater for the variable conductivity cases also in this 2-D study. Again a stronger subadiabatic character is found for the basal heating case near the lower boundary layer. The differences in η between constant and variable thermal conductivity are minor but one can recognize that the span of depths, where η hovers around 1, is smaller in Fig. 3 than in Fig. 1. Moreover, a slightly superadiabatic geotherm can be obtained for variable k and internal heating even below the upper boundary layer. This effect is caused by a low thermal conductivity at the base of the upper boundary layer due to its strong thermal dependence.

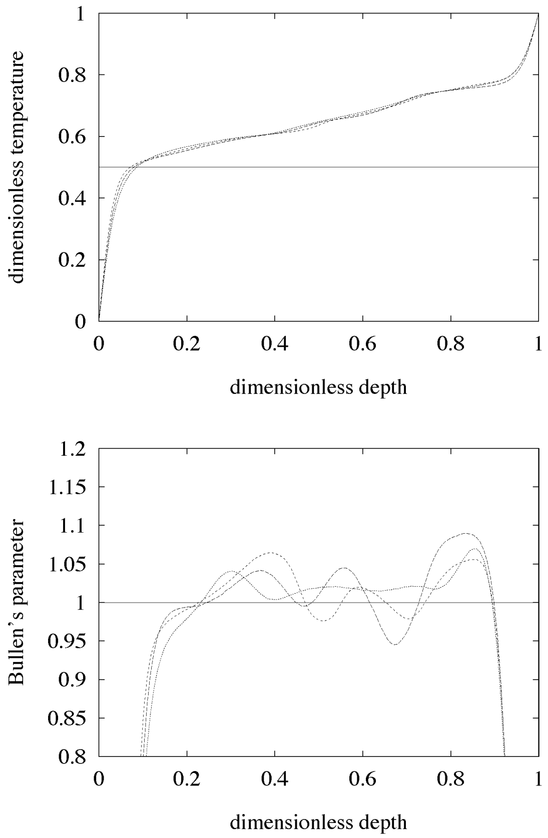

Fig. 2. Three snapshots of dimensionless horizontally averaged temperature $\langle T \rangle$ and the Bullen parameter η as a function of dimensionless depth z for the constant thermal conductivity $k=1$, constant thermal expansivity $\alpha=1$ and internal heating $R=8$. Otherwise, same as in Fig. 1.

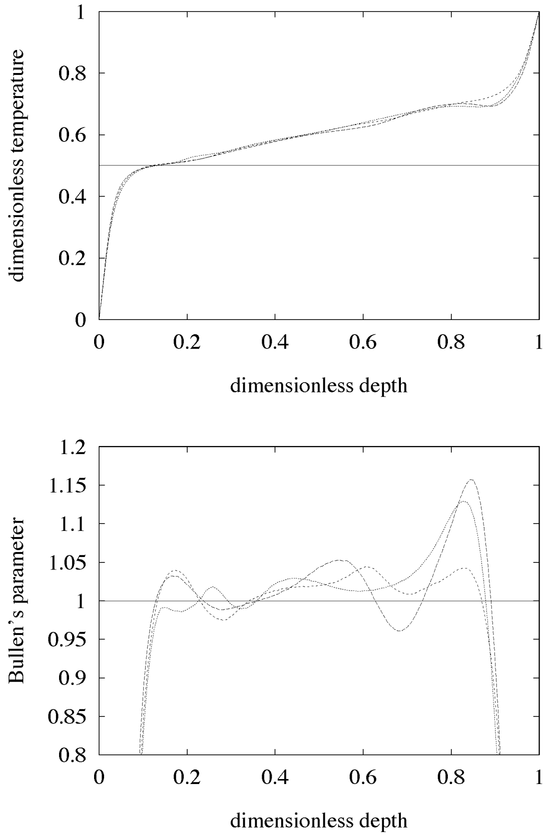

Fig. 3. Three snapshots of dimensionless horizontally averaged temperature $\langle T \rangle$ and the Bullen parameter η as a function of dimensionless depth z for the variable thermal conductivity k, see Eq. 4, constant thermal expansivity $\alpha=1$ and purely basal heating $R=0$. Otherwise, same as in Fig. 1.

The results for the depth-dependent thermal expansivity $\alpha(z)$ and constant thermal conductivity $k=1$ are in Figs. 5 and 6. These configurations thus reflect a decrease of buoyancy as well as of adiabatic heating/cooling with depth. Surprisingly, no internal heating mode $R=0$ results in subadiabatic geotherms below the upper boundary layer. The geotherms of the configuration with $R=8$ are much closer to an adiabat. These results demonstrate that the local character of a geotherm may be very sensitive to changes of the

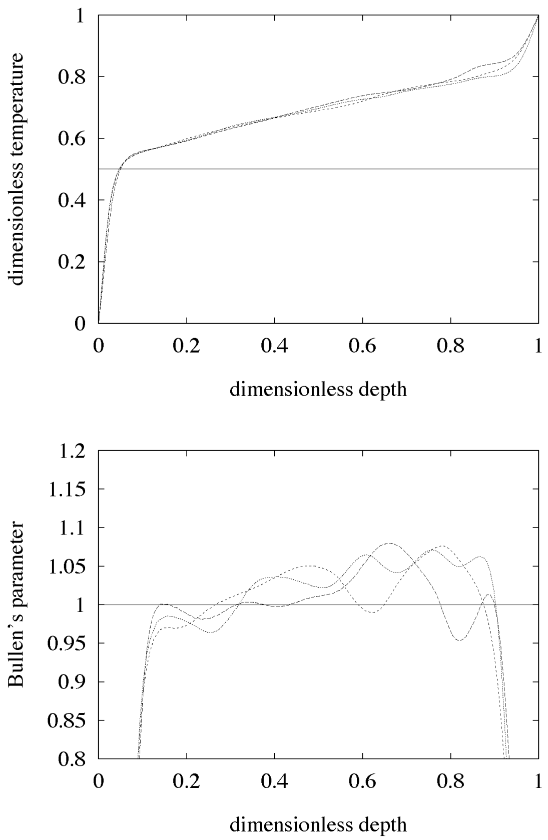

Fig. 4. Three snapshots of dimensionless horizontally averaged temperature $\langle T \rangle$ and the Bullen parameter η as a function of dimensionless depth z for the variable thermal conductivity k, see Eq. 4, constant thermal expansivity $\alpha = 1$ and internal heating $R = 8$. Otherwise, same as in Fig. 1.

mantle physical parameters. Notice also the decrease of the interior temperature from depth-dependent thermal expansivity [13].

In all cases the subadiabatic and the superadiabatic regions alternate with much bigger subadiabatic excursions mainly for the purely basal heating case. In short, we did not find a situation in which η remains close to 1 within a margin of a few percent. An interesting question arises as to the degree of accuracy of η current seismic models [24] can provide, since such information concerning η in the deep mantle was not provided in the PREM model [19]. Issues of resolution of η have not been provided in the recent models (e.g. [22,25]). More work in seismology would be needed to shed more light on these intriguing questions.

4. Concluding remarks

We have demonstrated with simple 2-D thermal convection models within the extended-Boussinesq framework that reasonable Bullen parameter profiles can be derived and that fluctuations of η, of the order of up to 10%, can be detected by an averaging depth scale of several hundred kilometers. Although our geotherms are more or less subadiabatic ($\eta > 1$) outside the boundary layers, there are also studies pointing to $\eta < 1$ in

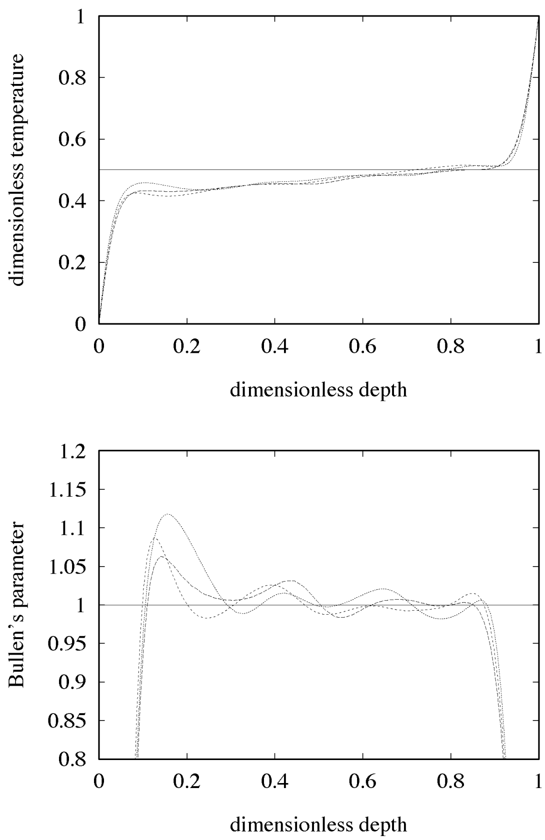

Fig. 5. Three snapshots of dimensionless horizontally averaged temperature $\langle T \rangle$ and the Bullen parameter η as a function of dimensionless depth z for the constant thermal conductivity $k = 1$, depth-dependent thermal expansivity $\alpha(z)$, see Eq. 5, and purely basal heating $R = 0$. Otherwise, same as in Fig. 1.

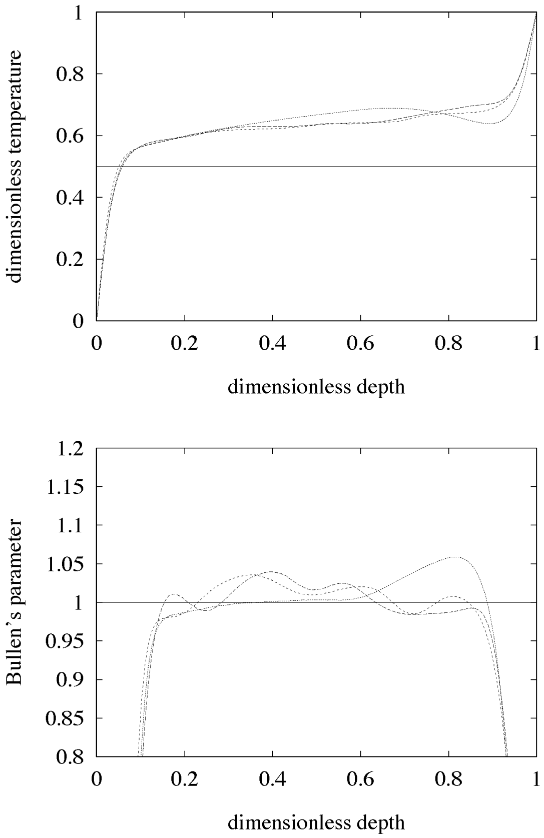

Fig. 6. Three snapshots of dimensionless horizontally averaged temperature $\langle T \rangle$ and the Bullen parameter η as a function of dimensionless depth z for the constant thermal conductivity $k=1$, depth-dependent thermal expansivity $\alpha(z)$, see Eq. 5, and internal heating $R=8$. Otherwise, same as in Fig. 1.

the deep mantle. For example, van den Berg and Yuen [26] showed that the bottom third of the lower mantle appears to be superadiabatic in the models with stiff lower mantle rheology. Similarly, a newly developed parameterization of the equation of state used in conjunction with experimental data on $MgSiO_3$ perovskite yields adiabatic lower mantle geotherms up to 1500 km depth and superadiabatic thereafter [27]. Such a conflict of ideas should be a stimulating challenge for further intensive research. We have just opened the door for η profiles to be employed in the future for constraining geodynamic scenarios. More work is needed to understand the role played by depth-dependent viscosity and phase transitions, as the models presented here show the potential of this approach, in that fluctuations of around 10% can be expected outside the boundary layers.

The issue of whether adiabaticity prevails in the bottom 1000 km of the lower mantle has also been raised by two recent developments. The first is the proposal by Kellogg et al. [15] that the lower mantle should be chemically stratified with enhanced radioactive heating. This proposed model would produce values of η greater than 1.1, because of its subadiabatic nature, due to a stagnant flow and rather strong internal heating (R around 20). Hansen and Yuen [28] found from thermal–chemical convection with moving heat sources whose strength is as strong as that used by Kellogg et al. [15] that the vertical temperature gradient can become zero and that there exists a zone with a negative temperature gradient. From Eq. 8 we can see that this situation would produce values of η much greater than 1.1. This is a substantial difference from the simple models presented in this study, which points to the potentially important role played by subadiabaticity of the lower mantle above D″ in discriminating between realistic and unrealistic convection models. The second is the finding by Ishii and Tromp [24] from free oscillation splitting data that the deep mantle is chemically heterogeneous. Such a situation in the vicinity of the D″ layer would produce significant superadiabatic deviations from adiabaticity, which can be assessed with thermal–chemical convection models using the extended-Boussinesq approximation [28,29].

Acknowledgements

We are grateful for discussions with Guy Masters, Ulli Hansen and Jerry Mitrovica. Constructive remarks from two anonymous reviewers are acknowledged. This research has been supported by Charles University Grant 170/1998/B-GEO/MFF and the Geosciences Program of the Department of Energy.***[RV]***

References

[1] G. Masters, Observational constraints on the chemical and thermal structure of the Earth's deep interior, Geophys. J. R. Astron. Soc. 57 (1979) 507–534.
[2] I. Jackson, Elasticity, composition and temperature of the Earth's lower mantle: a reappraisal, Geophys. J. Int. 134 (1998) 291–311.
[3] D.L. Anderson, Theory of the Earth, Blackwell Scientific, Boston, MA, 1989, 366 pp.
[4] C.R. Bina, P.G. Silver, Bulk sound travel times and implications for mantle composition and outer core heterogeneity, Geophys. Res. Lett. 24 (1997) 499–502.
[5] H. Jeffreys, The Earth, Cambridge University Press, Cambridge, 1976.
[6] K.E. Bullen, The Earth's Density, Chapman and Hall, London, 1975.
[7] V. Steinbach, D.A. Yuen, The non-adiabatic nature of mantle convection as revealed by passive tracers, Earth Planet. Sci. Lett. 136 (1995) 241–250.
[8] U. Christensen, D.A. Yuen, Layered convection induced by phase transitions, J. Geophys. Res. 90 (1985) 10,291–10,300.
[9] G.T. Jarvis, D.P. McKenzie, Convection in a compressible fluid with an infinite Prandtl number, J. Fluid Mech. 96 (1980) 515–583.
[10] V. Steinbach, U. Hansen, A. Ebel, Compressible convection in the earth's mantle: a comparison of different approaches, Geophys. Res. Lett. 16 (1989) 633–635.
[11] D.L. Turcotte, A.T. Hsui, K.H. Torrance, G. Schubert, Influence of viscous dissipation on Benard convection, J. Fluid Mech. 64 (1974) 369–374.
[12] P.L. Olson, H.A. Singer, Creeping plumes, J. Fluid Mech. 158 (1985) 511–538.
[13] U. Hansen, D.A. Yuen, S.E. Kroening, T.B. Larsen, Dynamical consequences of depth-dependent thermal expansivity and viscosity on mantle circulations and thermal structure, Phys. Earth Planet. Interact. 77 (1993) 205–223.
[14] A.M. Hofmeister, Mantle values of thermal conductivity and the geotherm from phonon lifetimes, Science 283 (1999) 1699–1706.
[15] L.H. Kellogg, B.H. Hager, R.D. van der Hilst, Compositional stratification in the deep mantle, Science 283 (1999) 1881–1884.
[16] B. Fornberg, A Practical Guide to Pseudospectral Methods, Cambridge University Press, Cambridge, 1996, 231 pp.
[17] A. Chopelas, R. Boehler, Thermal expansivity in the lower mantle, Geophys. Res. Lett. 19 (1992) 1983–1986.
[18] J.-P. Poirier, Introduction to the Physics of the Earth's Interior, Cambridge University Press, Cambridge, 1991, 264 pp.
[19] A.M. Dziewonski, D.L. Anderson, Preliminary reference Earth model, Phys. Earth Planet. Interact. 25 (1981) 297–356.
[20] T. Tanimoto, The Backus–Gilbert approach to three-dimensional structure in the upper-mantle II. SH and SV velocity, Geophys. J. R. Astron. Soc. 84 (1986) 49–69.
[21] G. Masters, Low-frequency seismology and the three-dimensional structure of the Earth, Phil. Trans. R. Soc. London 328 (1989) 329–349.
[22] L. Boschi, A.M. Dziewonski, High- and low-resolution images of the Earth's mantle: Implications of different approaches to tomographic modeling, J. Geophys. Res. 104 (1999) 25,567–25,594.
[23] F. Dubuffet, D.A. Yuen, M. Rabinowicz, Effects of a realistic mantle thermal conductivity on the patterns of 3-D convection, Earth Planet. Sci. Lett. 171 (1999) 401–409.
[24] M. Ishii, J. Tromp, Normal-mode and free-air gravity constraints on lateral variations in velocity and density of Earth's mantle, Science 285 (1999) 1231–1236.
[25] H.-W. Zhou, A high resolution P wave model for the top 1200 km of the mantle, J. Geophys. Res. 101 (1996) 27791–27810.
[26] A.P. van den Berg, D.A. Yuen, Modelling planetary dynamics by using the temperature at the core–mantle boundary as a control variable: effects of rheological layering on mantle heat transport, Phys. Earth Planet. Interact. 108 (1998) 219–234.
[27] C.R.S. da Silva, R.M. Wentzcovitch, A. Patel, G.D. Price, S.I. Karato, The composition and geotherm of the lower mantle: constraints from the elasticity of silicate perovskite, Phys. Earth Planet. Interact. 118 (2000) 103–109.
[28] U. Hansen, D.A. Yuen, Extended-Boussinesq thermal–chemical convection with moving heat sources, Earth Planet. Sci. Lett., (2000) in press.
[29] U. Hansen, D.A. Yuen, Dynamical influences from thermal–chemical instabilities at the core–mantle boundary, Geophys. Res. Lett. 16 (1989) 629–632.